THE EVALUATION OF THE INTERSLICE SIDE FORCES FOR SLOPE STABILITY ANALYSIS BY THE FINITE ELEMENT METHOD

by

G. WARD WILSON, P. ENG.
Clifton Associates Ltd., Consulting Geotechnical Engineers, Saskatoon, Saskatchewan

and

D. G. FREDLUND
Professor of Civil Engineering

Department of Civil Engineering
University of Saskatchewan
Saskatoon, Saskatchewan
Canada S7N OWO

Presented at the
Ninth Canadian Congress of Applied Mechanics
(CANCAM 83)
College of Engineering
University of Saskatchewan
Saskatoon, Canada

May 30 - June 3, 1983

THE EVALUATION OF THE INTERSLICE SIDE FORCES FOR SLOPE STABILITY ANALYSIS BY THE FINITE ELEMENT METHOD

ABSTRACT

The method of slices for limiting equilibrium analysis has an inherent problem of static indeterminancy. That is, the number of unknowns exceeds the number of equations available to obtain a solution. A solution requires either additional physics or assumptions to render the analysis determinant. In general, the latter has been found to be the most practical alternative.

The most commonly utilized assumptions are those regarding the direction of the interslice side forces. Difficulties resulting from the assumption used for the interslice side forces frequently occur. These are, either failure to converge to a solution for the factor of safety, or failure to obtain a physically admissible solution.

The direction of the interslice side forces were evaluated using a two-dimensional constant strain finite element analysis. Four slope inclinations were investigated, ranging from moderately steep (i.e., three horizontal to one vertical to very steep (i.e., one horizontal to two vertical). The distributions of the interslice side force ratio, X/E, were found to be bell-shaped. The bells were flattest for the three horizontal to one vertical slope and sharpest for the one horizontal to two vertical slope. The peak values of the interslice side force ratio, X/E, occur at midslope. In addition, points of inflection in the curvature were observed just slightly beyond the crest and the toe of slope. These observations were used as

a criteria to develop a generalized function which simulates the distributions of the interslice side force ratio, X/E.

INTRODUCTION

Geotechnical engineers are often asked to quantatively evaluate the stability of a natural or man-made slope. A large selection of techniques are available for the analysis of slope stability problems. The most frequently utilized numerical procedure is the methods of slices.

The methods of slices subdivide the soil mass into a series of vertical slices and applies the principles of limiting equilibrium. A factor of safety is obtained by resolving the forces acting on each slice through an iterative procedure. The methods of slices are statically indeterminate and require an assumption in order to compute the factor of safety. Difficulties sometimes arise as a result of these assumptions. For example, the solution may not converge. The convergence problems are related to the assumption made regarding the internal forces acting within the soil mass.

This paper uses an elastic theory approach (i.e., the finite element method) to evaluate the internal forces acting within four selected slope geometries. More specifically, the directions of the interslice shear and normal side forces are computed using the finite element method. The object of this research is to determine a generalized function which will predict a realistic direction for the interslice side forces.

THE METHOD OF SLICES FOR SLOPE STABILITY ANALYSIS

The method of slices first requires the selection of a potential slip surface. The soil above this slip surface is perceived as a series of individual free bodies while the soil beneath is considered perfectly rigid. The forces acting on each slice are evaluated using the principles of statics and the Mohr-Coulomb failure criteria. A factor of safety is computed for moment and/or force equilibrium.

Numerous procedures for the method of slices have been developed. The most commonly used procedures are:

1). The Ordinary or Fellenius method.

2). The simplified Bishop method.

3). The Spencer method.

4). The Janbu simplified method.

5). The Janbu generalized method.

6). The Lowe and Karafiath method.

7). The Corps of Engineers method.

8). The Morgenstern-Price method.

9). The General Limit Equilibrium method.

Some of these procedures satisfy all conditions of statics whereas some only partially satisfy static equilibrium.

Two elements of statics must be satisfied for complete equilibrium. These are:

1). the summation of moments about an arbitrary point must equal zero, and,

2). the summation of forces in two othogonal directions must equal zero.

Only four of the methods listed above satisfy complete equilibrium. These are the Spencer, Janbu Generalized, Morgenstern-Price and General Limit Equilibrium Methods. The General Limit Equilibrium is a formulation which embraces all the methods listed above, except the Ordinary method (Fredlund, Krahn and Pufahl, 1981). Therefore, the formulation of this method has been chosen to illustrate the method of slices.

Figure 1 illustrates the forces and variables which are utilized in the derivation of the equilibrium equations. The definitions are as follows:

W = the total weight of the slice of height 'h' and width 'b'.

P = the total normal force acting at the base of slice over the length 'ℓ'.

S_m = the shear force mobilized at the base of the slice over the length 'ℓ'.

E_L, E_R = the total horizontal interslice normal forces, on the left and right sides of the slice, respectively.

X_L, X_R = the total vertical interslice shear forces, on the left and right sides of the slice, respectively.

R = the radius or moment arm associated with the mobilized shear force, S_m.

x_c = the horizontal distance from the centroid of the slice to the center of rotation.

f = the perpendicular offset of the normal force from the center of rotation.

A_L, A_R = the external water forces, on the left and right extremities of the slip surface, respectively.

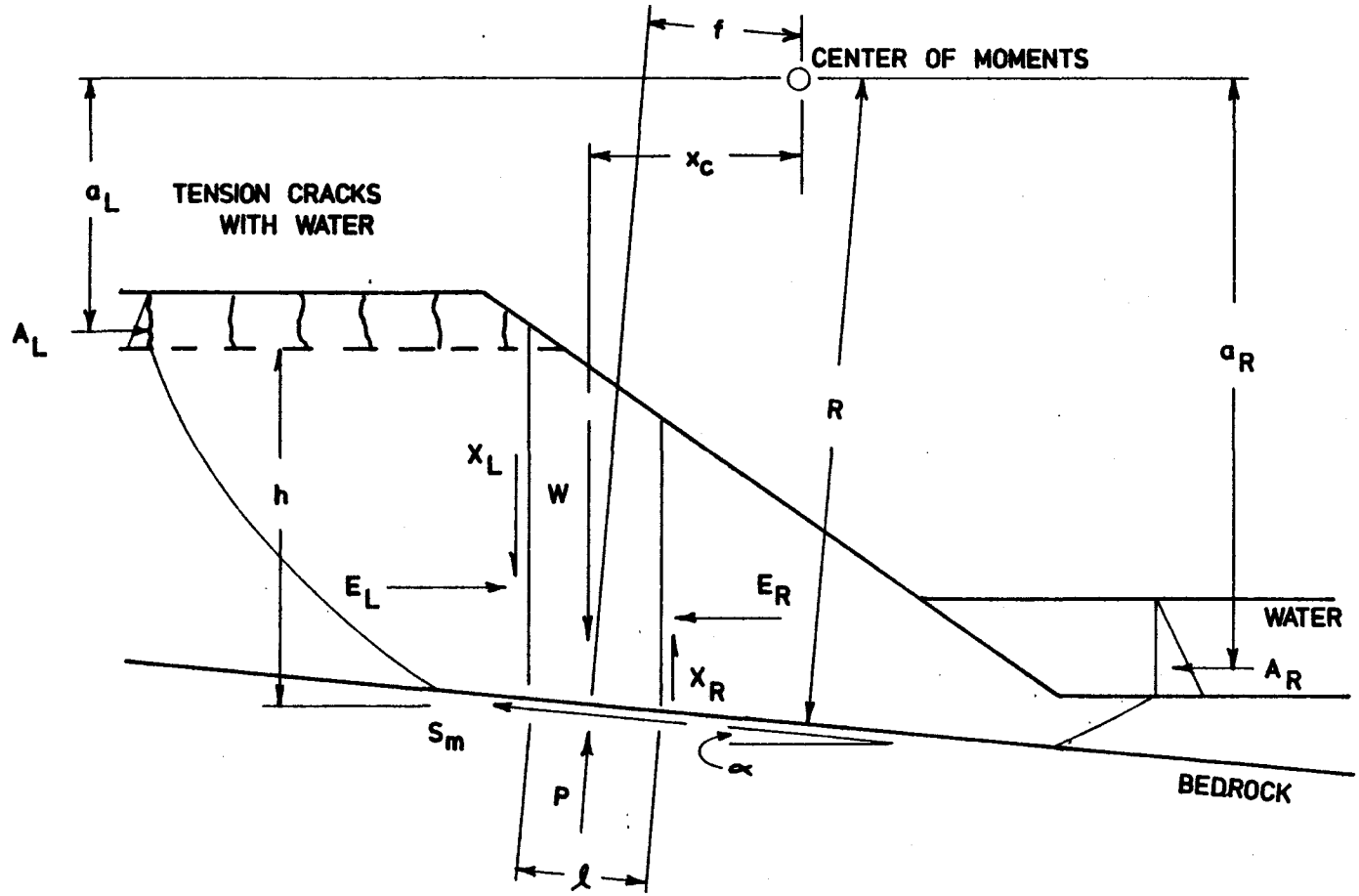

FIGURE 1 FORCES ACTING FOR THE METHOD OF SLICES
(GENERALIZED LIMIT EQUILIBRIUM METHOD)

a_L, a_R = the perpendicular distance from the resultant external water force to the center of rotation, on the left and right extremities of the slip surface, respectively.

α = the angle between the tangent to the center of the base of the slice and the horizontal.

Two equilibrium equations are utilized to compute the factor of safety. For moment equilibrium,

$$F_m = \frac{\Sigma[c'\ell + (P - u\ell) \tan \emptyset'] R}{\Sigma Wx - \Sigma Pf \pm Aa} \qquad (1)$$

where:

F_m = factor of safety with respect to moment equilibrium.

c' = the effective cohesion intercept.

$\emptyset'$ = the effective angle of internal friction.

u = the pore-water pressure.

ℓ = the length of the failure surface at the base of the slice.

For horizontal force equilibrium,

$$F_f = \frac{\Sigma[c'\ell + (P - u\ell) \tan \emptyset'] \cos\alpha}{\Sigma P \sin\alpha \pm A} \qquad (2)$$

where:

F_f = factor of safety with respect to force equilibrium.

The normal forces acting on the base of each slice are computed summing forces vertically on each slice which gives:

$$P = \frac{W - (X_R - X_L) - \frac{c'\ell \sin\alpha}{F} + \frac{u\ell \tan\phi' \sin\alpha}{F}}{m_\alpha} \quad (3)$$

where:

$$m_\alpha = \cos\alpha + \frac{\sin\alpha \tan\phi'}{F} \quad (4)$$

F = the factor of safety with respect to either moment or force equilibrium depending on which factor of safety equation is being solved.

The solution to the equilibrium equations requires an assumption with respect to the direction of the resultant interslice side forces. This is mathematically described as follows:

$$X/E = \lambda f(x) \quad (5)$$

where:

f(x)= a functional form which describes the general change in slope of the resultant interslice forces across the slope (Figure 2).

λ = a constant representing the percentage of the function used when solving for the factor of safety.

The magnitudes for the interslice normals, E, are obtained by summing forces horizontally on each slice (Morgenstern and Price, 1965) as follows:

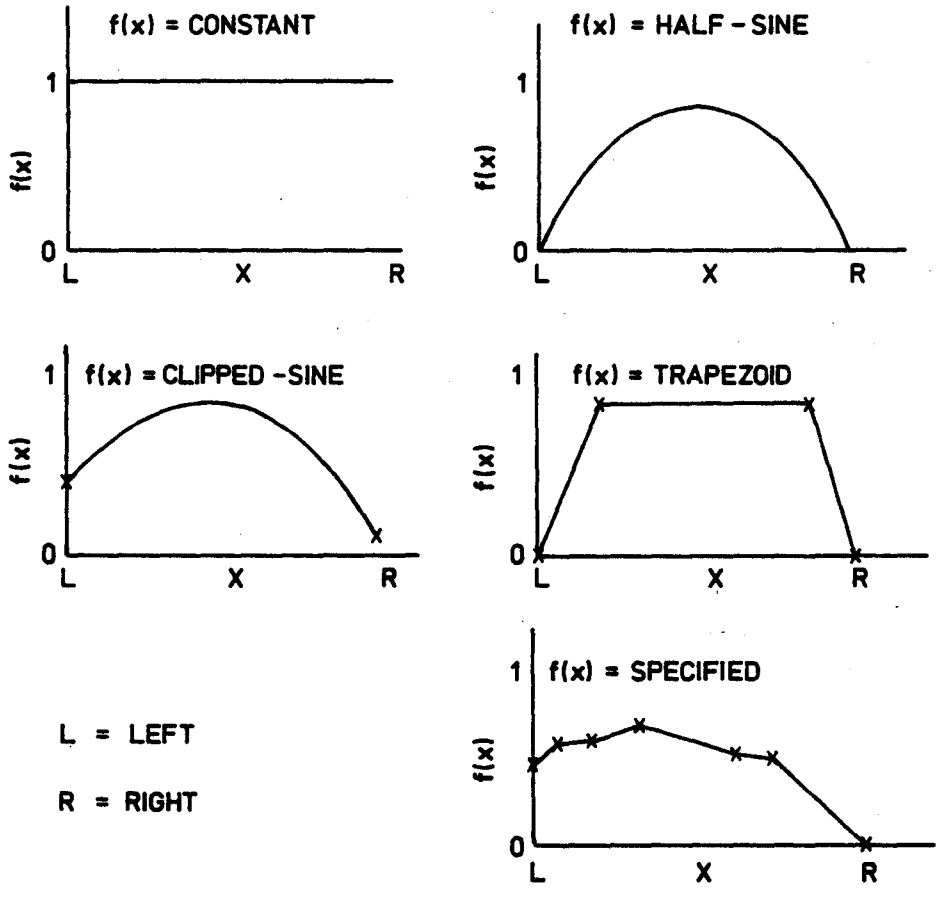

FIGURE 2 FUNCTIONAL FORMS COMMONLY USED IN ANALYSIS

$$E_R - E_L = \{W - (X_R - X_L)\} \tan\alpha - \frac{Sm}{\cos\alpha} \qquad (6)$$

DIFFICULTIES ENCOUNTERED WITH STATIC INDETERMINANCY

The method of slices for slope stability analysis has an inherent problem of static indeterminacy. The number of equations available for a solution is exceeded by the number of unknowns. Table 1 illustrates the number of unknowns and the number of equations utilized for a solution.

The condition of static indeterminancy may be resolved by utilizing either additional physics or assumptions regarding the interslice side forces. The use of an assumption for the direction of the interslice side forces has been the most commonly adopted approach. However, there are often difficulties associated with the assumed interslice functional relationships. These difficulties often appear in the following form:

1). A failure to achieve a solution which is physically admissible (i.e., the resultant interslice shear forces violate the failure criterion).

or,

2). A failure to produce a reasonable location for the line of thrust within the soil mass.

or,

3). A failure to converge to a solution within a reasonable number of iterations.

Table 1 Summary of Equations and Unknowns Associated with Complete Equilibrium.

---

n = number of slices

Equations	(for n slices)	
n	Mohr Coulomb Failure equations	
n	Moment Equilibrium equations	
n	Vertical force equilibrium equations	
n	Horizontal force equilibrium equations	
4n	Total equations	
Unknowns	(for n slices)	
1	Factor of safety	
1	Value of Lamba (λ)	
n	Normal forces acting on the base of each slice (P)	
n	Locations of the normal forces (P)	
n	Shear forces acting on the base of each slice (S_m)	
n-1	Interslice normal forces (E)	Interslice resultant forces (Q)
	OR	
n-1	Interslice shear forces (X)	Directions of the resultant forces (Q).
n-1	Locations of application for interslice forces	
6n-1	Total unknowns	

Failure to converge to a solution which is physically admissible is the most common problem. Ironically, the computed factor of safety may be relatively insensitive to the assumed side force function as long as the solution converges. Tensile internal forces which violate the Mohr-Coulomb failure criteria, are occasionally computed within some solutions which indicate a deficiency in the analysis.

The inability to converge upon a solution frequently plagues methods which attempt to satisfy all conditions of equilibrium. Sariano (1976) studies the "existance and uniqueness of solutions" in methods of slope stability analysis. It was pointed out that an assumption such as parallel side forces is not compatible with equilibrium conditions for steep and highly cohesive slopes. Ching (1981) in a comprehensive study concluded "convergence problems are often encountered in analyzing steep and highly cohesive slopes". It was suggested that the selection of a proper side force function is of "paramount importance" in the analysis of steep slopes when using methods which completely satisfy all conditions of equilibrium.

FINITE ELEMENT ANALYSIS OF SIMPLE SLOPES

The Finite element method was used to investigate the internal stresses acting within four simple slope geometries. The slope inclinations investigated were:

1. Three horizontal to one vertical; 3:1.
2. Two horizontal to one vertical; 2:1.
3. One horizontal to one vertical; 1:1.
4. One horizontal to two vertical; 1:2.

Only circular slip surfaces have been considered. The slope geometries investigated were considered as homogeneous, linear elastic continuums

deforming under gravity. The analyses were performed using a Digital Corporation computer, model VAX 11/780, available at the University of Saskatchewan, Saskatoon, Canada.

The finite element method adopted for the stress analysis uses two-dimensional, constant strain triangular elements. The element stiffness matrix for this analysis is given as:

$$\{\underline{Sx}\ \underline{Sy}\} = \int [B]^T [C]\ [B]\ dv\ \{\underline{u}\ \underline{v}\} \qquad (7)$$

where,

[B] = The matrix relating displacement at the nodes to element strain.

[C] = The matrix describing the constitutive relationship for 2-dimensional, plane strain.

$\underline{Sx}$ and $\underline{Sy}$ = forces at the nodes in the x and y directions, respectively.

$\underline{u}$ and $\underline{v}$ = displacements at the nodes in the x and y directions, respectively.

The formulation of this approach is well known and has been discussed by many (Desai, 1979; Zienkiewicz, 1977).

The internal stresses or forces of interest were the horizontal normal, E, and vertical shear, X, forces acting on the sides of vertical slices within the potential sliding mass. These forces are obtained by integration of stress over the length of the vertical section.

$$E = \int_a^b \sigma_x \, y \, dy \tag{8}$$

$$X = \int_a^b \tau_{xy} \, y \, dy \tag{9}$$

Figure 3, illustrates the above expressions.

Average nodal stresses were used to compute the normal, E, and shear, X, forces acting along vertical sections above the slip surfaces. Simpson's method of integration was utilized for the integration. Following the computation of the total normal, E, and shear, X, forces, a functional relationship describing the directions of the resultant interslice side forces was computed.

$$f(x) = X/E \tag{10}$$

Two triangular finite element meshes were used for the analysis of each slope. A large coarse mesh was first constructed to maintain the boundaries at an adequate distance from the slope to minimize their influence. A second finer mesh was constructed for the region within the immediate region of the slope. Displacements computed within the coarser mesh were applied as boundary conditions for the analysis of the fine mesh. Figure 4 and 5 illustrates the meshes used for the three horizontal to one vertical slope inclination.

A linear elastic finite element analysis of the slope inclinations modelled required the selection of three material properties, Young's Modulus of elasticity, unit weight of material, and Poisson's ratio. The following material properties were selected and used within the analyses:

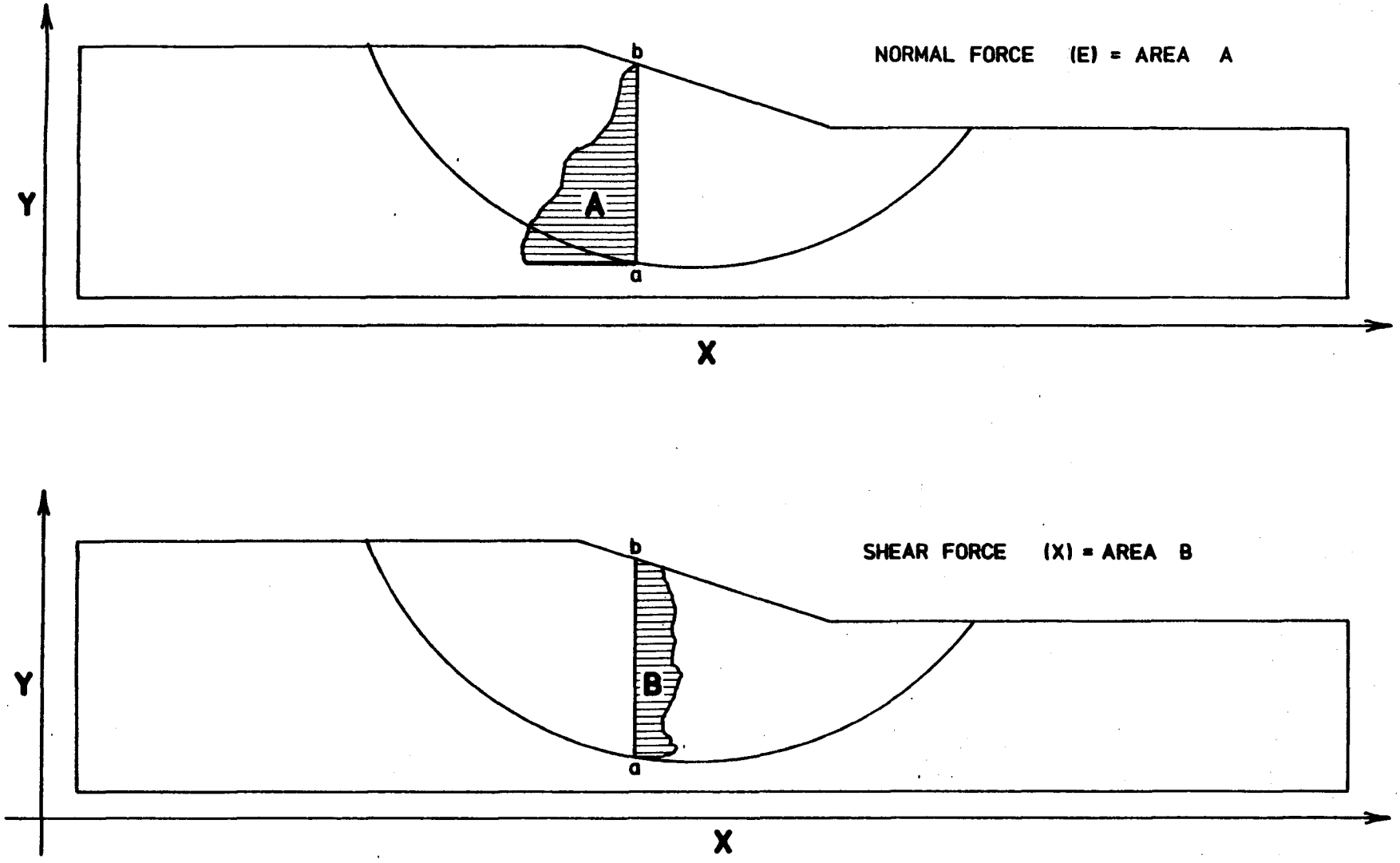

FIGURE 3 THE NORMAL AND SHEAR FORCES ACTING ACROSS A TYPICAL SECTION THROUGH A POTENTIAL SLIDING MASS

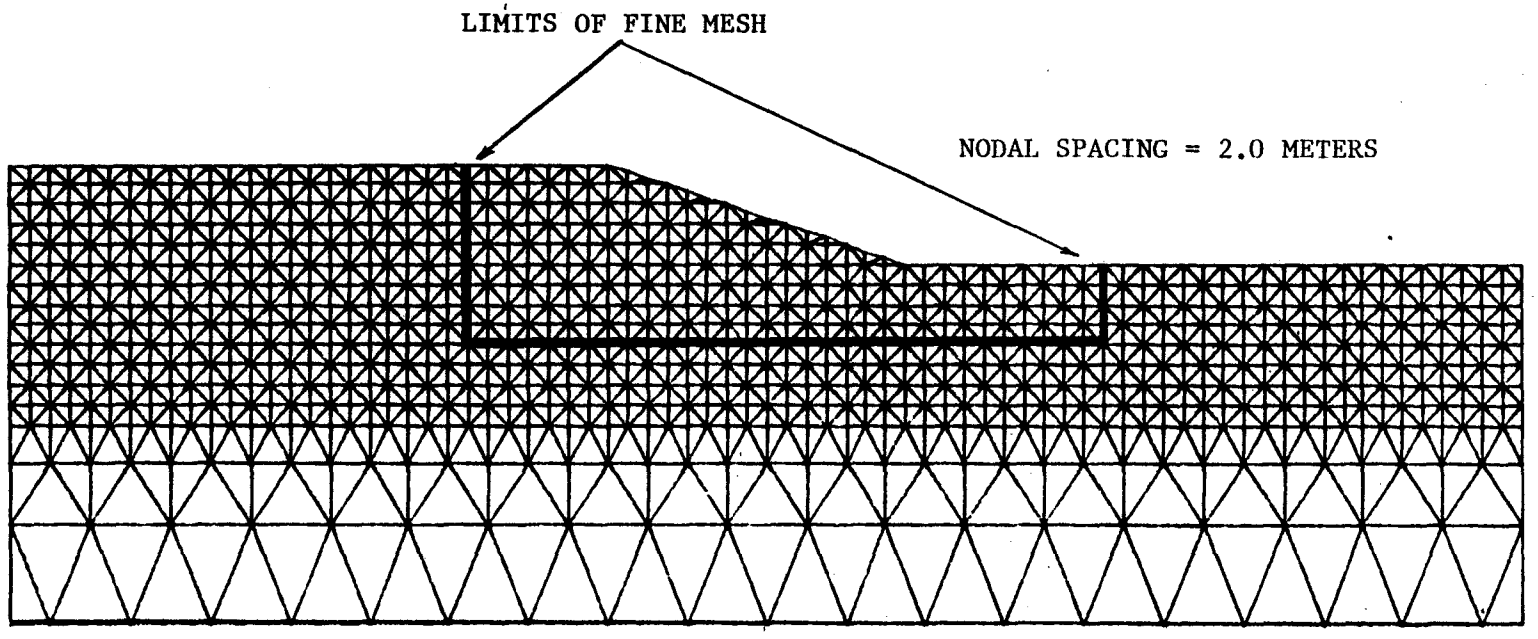

FIGURE 4 THE COARSE FINITE ELEMENT MESH FOR THE THREE HORIZONTAL TO ONE VERTICAL SLOPE

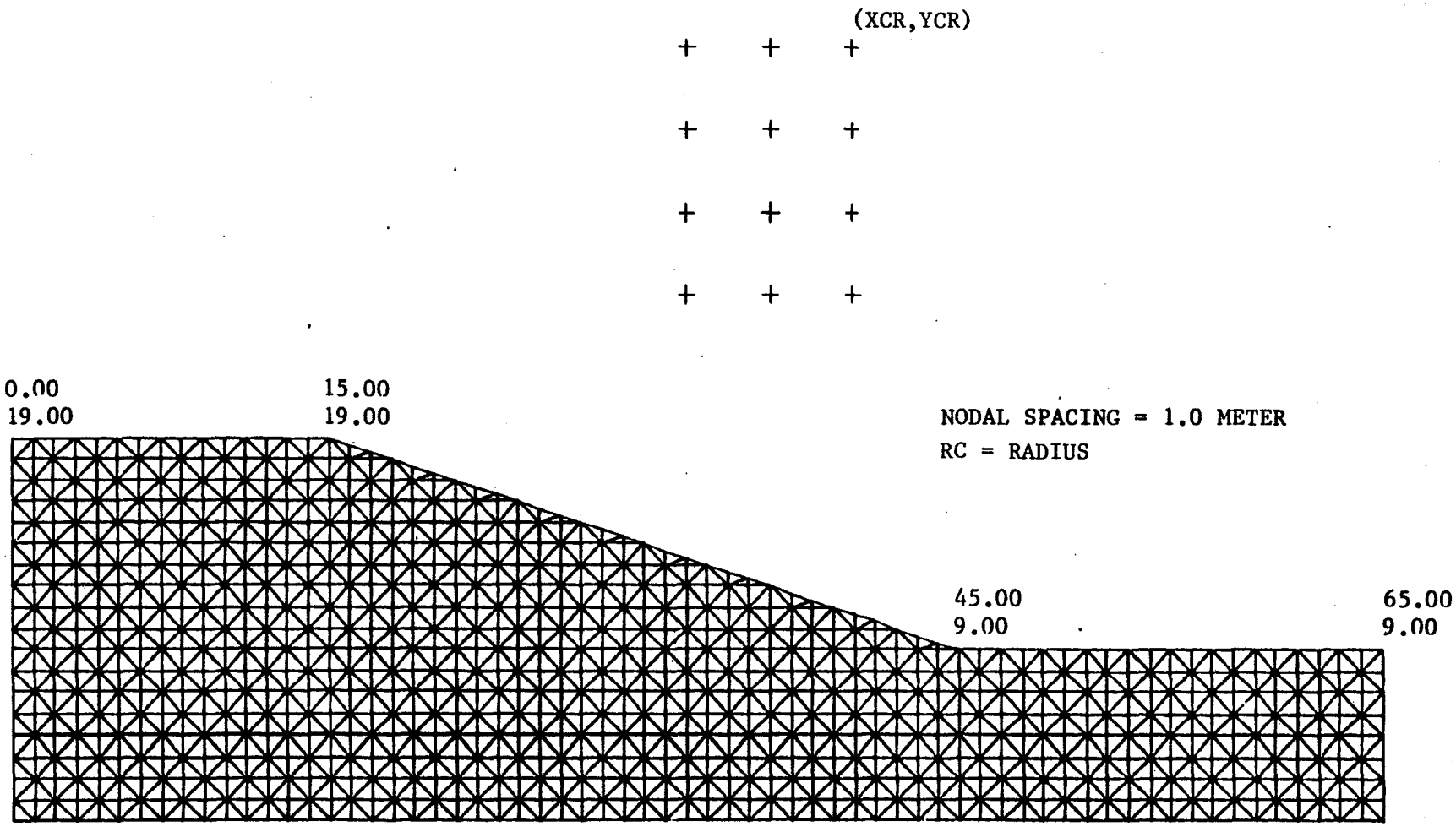

FIGURE 5 THE FINE FINITE ELEMENT MESH FOR THE THREE HORIZONTAL TO ONE VERTICAL SLOPE

1). Young's modulus of elasticity, E = 15,000 kPa.

2). Unit weight of material, γ = 18.0 kN/M^3.

3). Poisson's ratio, μ = 0.40.

Although the selection of elastic properties is an important consideration within an elastic stress analysis, they are considered to be secondary for this particular investigation. The ratio of internal forces are primarily a function of gravity and geometry and are relatively independent of displacements.

PRESENTATION OF RESULTS

The interslice side force ratios, X/E, were computed for each of the four slopes. A wide range of circular slip surfaces were investigated for each slope by varying the center of rotation and the radius for the slip surfaces. A total of 228 different slip surfaces were investigated. Figures 6a through 6d illustrate the distributions of the interslice side force ratio, X/E, typically observed.

DISCUSSION AND ANALYSIS

The distributions of the interslice side force ratio, X/E, are bell-shaped for the four slope geometries investigated. The bells were observed to be flattest for the shallow slopes and sharpest for the steep slopes. The value of the interslice side force ratio, X/E, is relatively constant between the crest and toe of slope for both the 3:1 and 2:1 slopes. Sharp peaks occur at midslope for the 1:1 and 1:2 slopes. These peaks are sharpest when the slip surface is shallow seated.

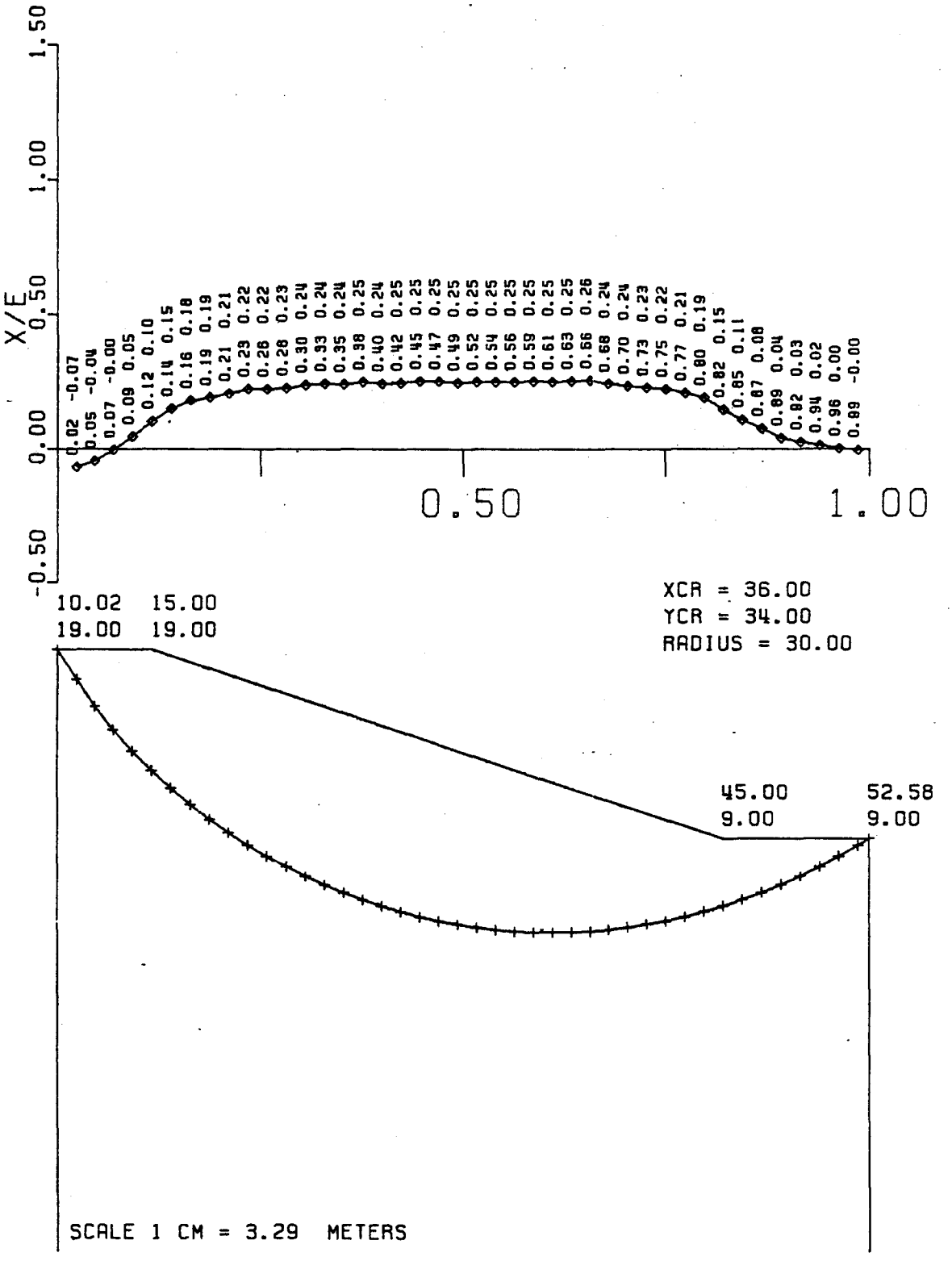

FIGURE 6a THE INTERSLICE SIDE FORCE RATIO (X/E) DISTRIBUTION FOR A DEEP SEATED SLIP SURFACE IN THE THREE HORIZONTAL TO ONE VERTICAL SLOPE

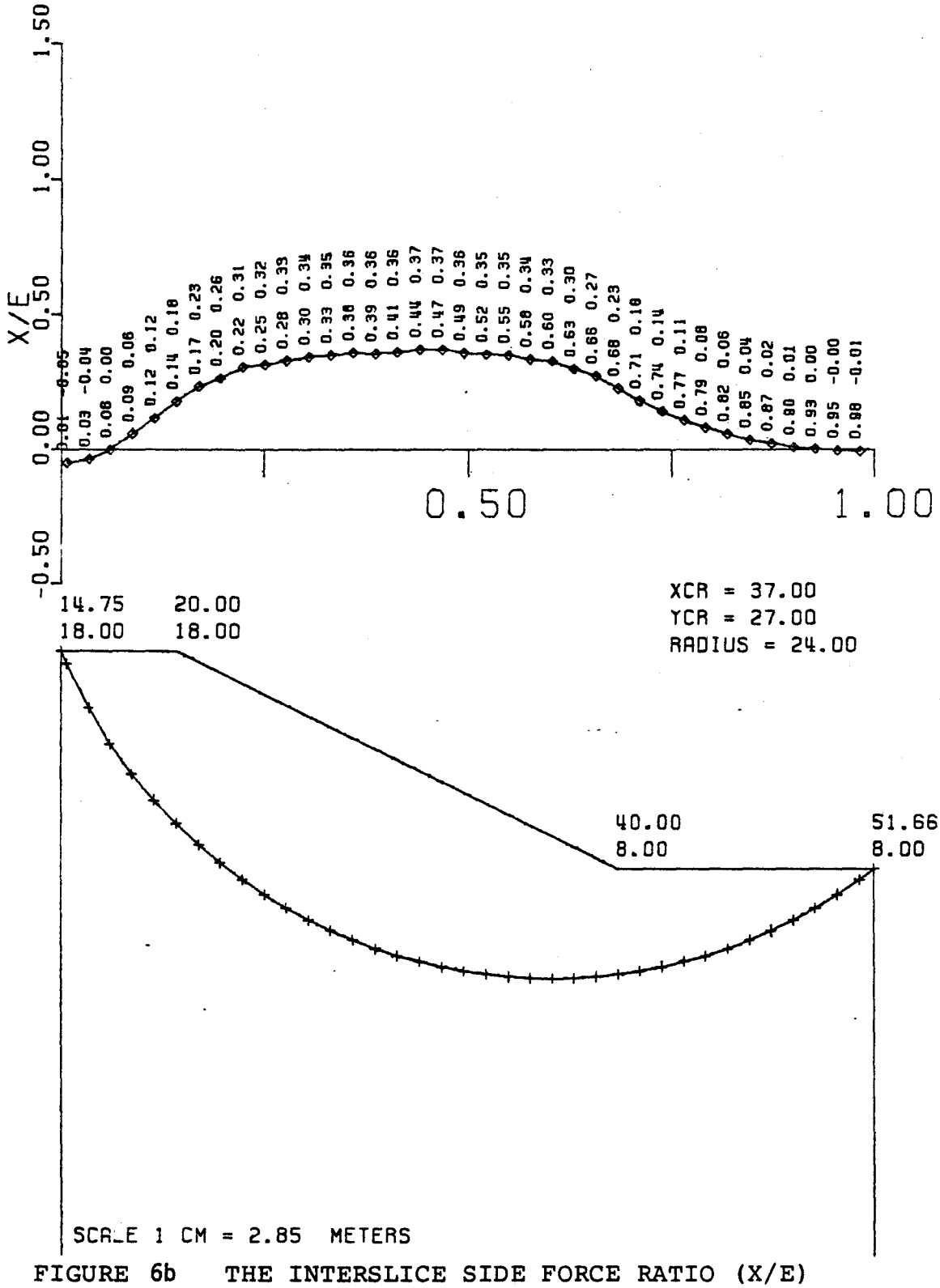

FIGURE 6b THE INTERSLICE SIDE FORCE RATIO (X/E) DISTRIBUTION FOR A DEEP SEATED SLIP SURFACE IN THE TWO HORIZONTAL TO ONE VERTICAL SLOPE

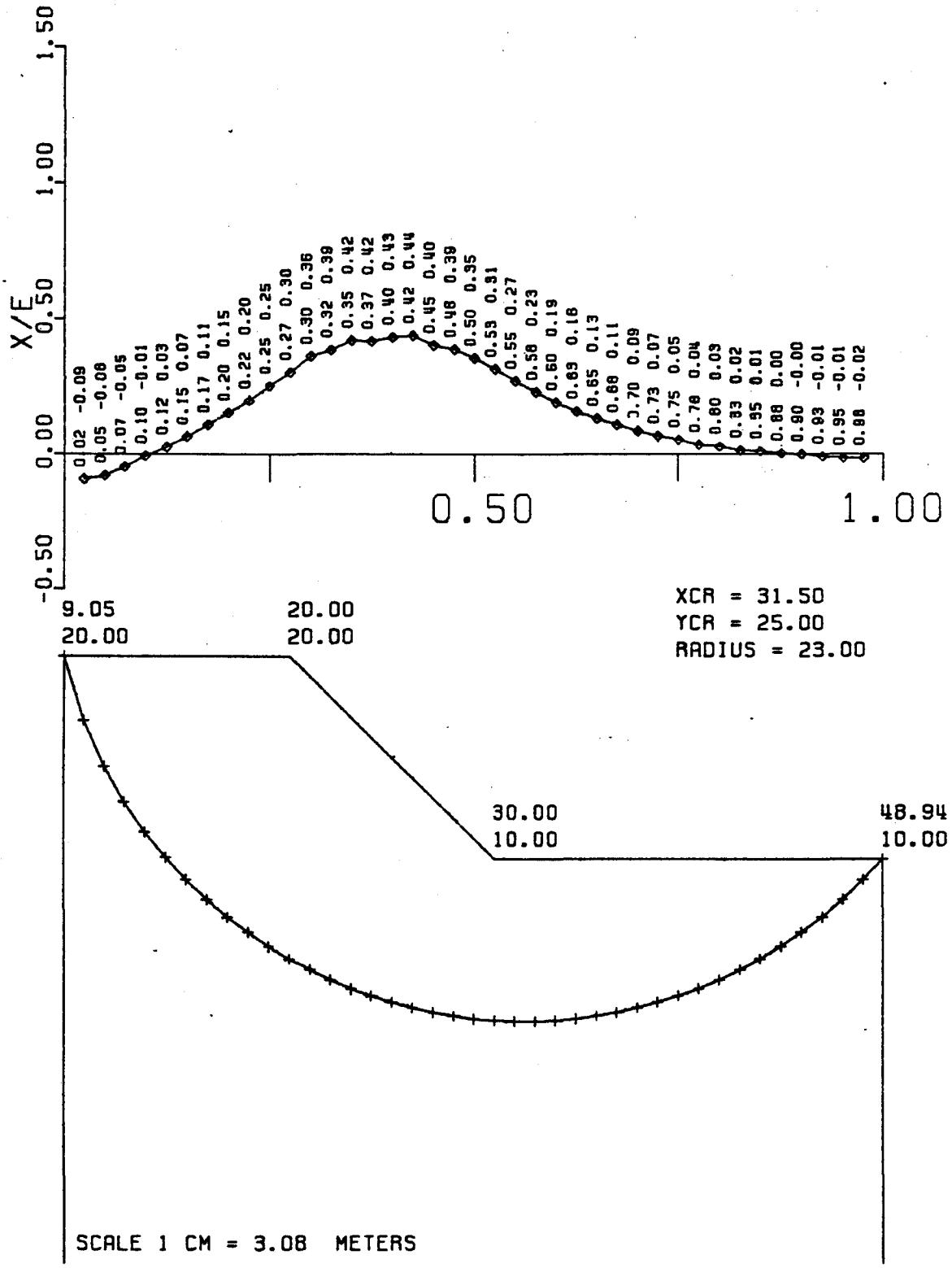

FIGURE 6c THE INTERSLICE SIDE FORCE RATIO (X/E) DISTRIBUTION FOR A DEEP SEATED SLIP SURFACE IN THE ONE HORIZONTAL TO ONE VERTICAL SLOPE

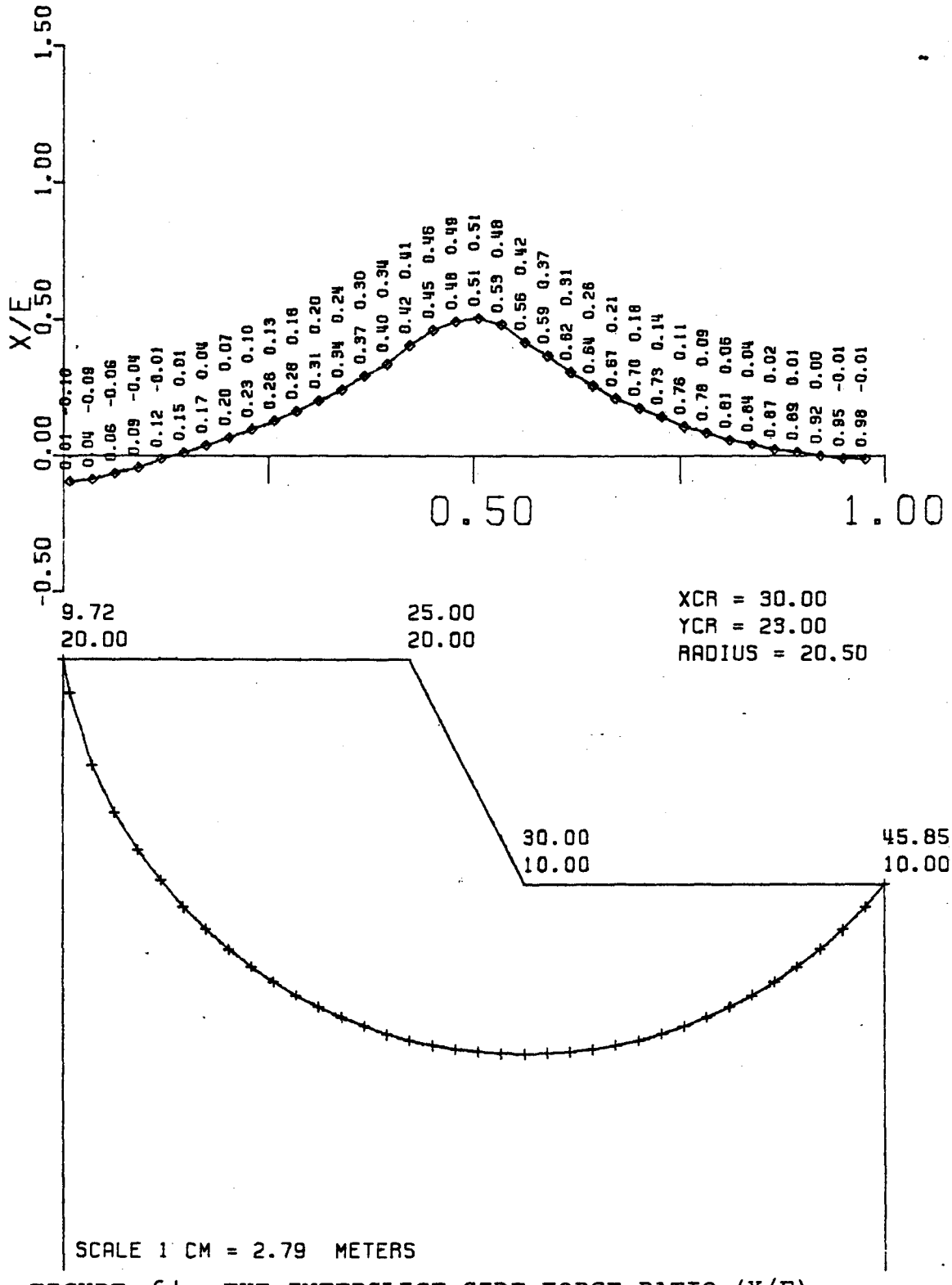

FIGURE 6d THE INTERSLICE SIDE FORCE RATIO (X/E) DISTRIBUTION FOR A DEEP SEATED SLIP SURFACE IN THE ONE HORIZONTAL TO TWO VERTICAL SLOPE

The curved distributions of the shear to normal force ratio, X/E, across the slopes show points of inflection to be near the crest and toe of the slopes. Four dimensionless variables, ω, ω_c, ω_t and ω_a, were adopted to define the locations of the inflection points relative to the middle of each slope. The definitions of these parameters are shown in Figure 7. The value 'ω_a' is defined as the mean distance to the inflection points measured from the mid-point of the slope. In general, the inflection points occur just beyond either the crest or the toe of the slope at an average distance of 0.069H, where H is the height of the slope.

The maximum values of the interslice side force ratio, X/E, were observed to always occur at midslope, halfway between the crest and the toe. Furthermore, the maximum values of the interslice side force ratio, X/E, approaches the tangent of the slope angle for shallow slip surfaces. Figure 8 shows values of the interslice side force ratio, X/E, versus the depth factor (d) for each of the four slopes investigated. The magnitude of the interslice side force ratio, X/E, at midslope versus the Depth Factor, D, plot as straight lines on a semi-log scale. The points plotted for each line shown on Figure 8 correspond to several slip surfaces defined by three centers of rotation for each slope inclination.

NUMERICAL SIMULATION OF THE DISTRIBUTION OF THE INTERSLICE SIDE FORCE RATIOS, X/E, COMPUTED BY FINITE ELEMENT

The distributions of the interslice side force ratios, X/E, are bell-shaped. A generalized function which simulates a simple bell-shaped curve is,

$$f(x) = e^{-\frac{1}{2} x^n} \qquad (11)$$

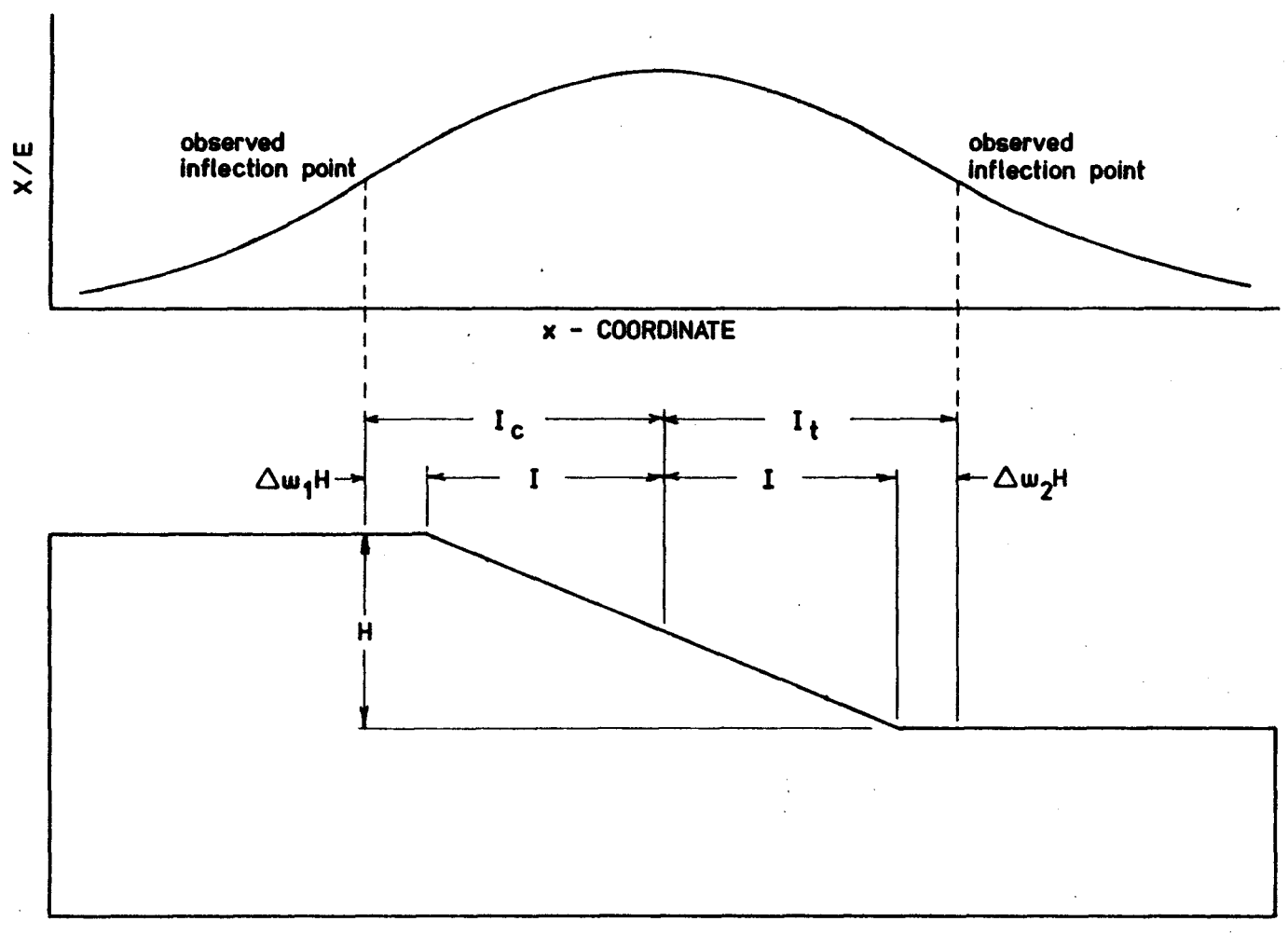

n = no. of observations

$$\omega = \frac{I}{H}$$

$$\omega_c = \frac{I_c}{H}$$

$$\omega_t = \frac{I_t}{H}$$

$$\Delta\omega_1 = \frac{\Sigma(\omega_c - \omega)}{n}$$

$$\Delta\omega_2 = \frac{\Sigma(\omega_t - \omega)}{n}$$

$$\omega_a = \frac{(\Delta\omega_1 + \Delta\omega_2)}{2}$$

FIGURE 7 THE DEFINITIONS OF THE DIMENSIONLESS VALUES 'ω', 'ω_c', 'ω_t' and 'ω_a'

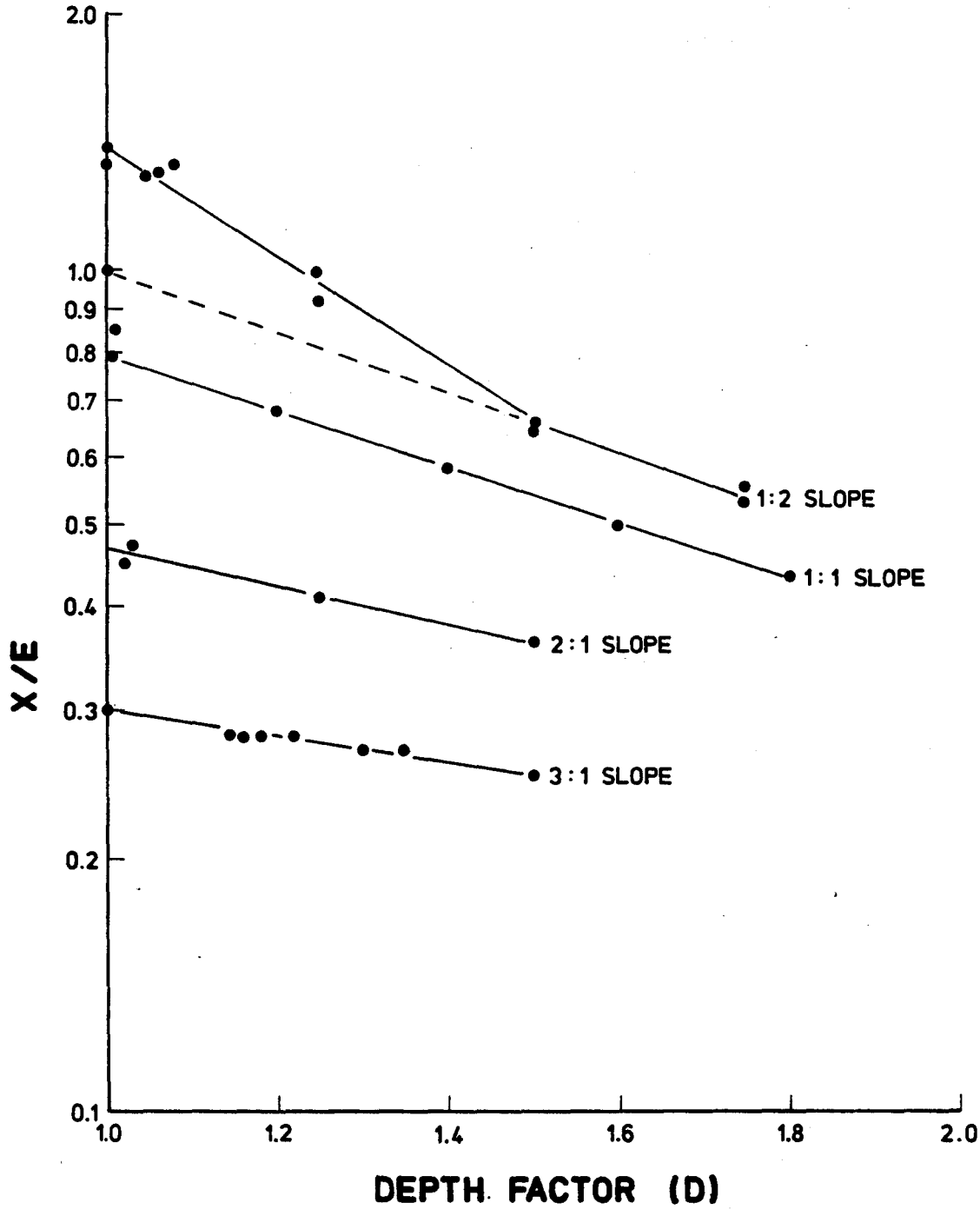

FIGURE 8 THE INTERSLICE SIDE FORCE RATIO (X/E) AT MIDSLOPE VERSUS THE DEPTH FACTOR (D)

were:

f(x) = The interslice side force ratio, X/E, at a given dimensionless x - co-ordinate.

x = The horizontal position relative to the center of the slope.

n = A power which dictates the flatness or sharpness of curvature.

This function is simialr to a normal distribution curve when n is equal to 2. The value of the power of n to simulate the finite element interslice side force ratios was determined by trial and error to give the most suitable curvature for each slope. These are:

1). 3:1 slope, n = 6.

2). 2:1 slope, n = 4.

3). 1:1 slope, n = 2.

4). 1:2 slope, n = 2.

Upon selection of the appropriate functional form, it is necessary to introduce variables which control the lateral and vertical limits of the bell-shaped curves. The inflection points were selected to define the lateral limits of the curves, and the generalized function is modified such that the inflection points occur as observed. This is accomplished by introducing a variable 'c' which when multiplied by the horizontal position 'x' gives a root 'R' to the second derivative of equation 11. The second derivative of equation 11 is:

$$f''(x) = \left(\frac{n^2 x^{2n-2}}{4} - \frac{n(n-1)x^{n-2}}{2}\right) e^{-\frac{1}{2}x^n} \qquad (12)$$

The roots 'R' of equation 12 for the values of 'n' previously given are:

1). for n=6, R = ± 1.0889

2). for n=4, R = ± 1.1067

3). for n=2, R = ± 1.0000

The positions of the inflection points relative to the middle of the slope are set equal to the root of equation 11 by the following expression:

$$R = c\omega_i \tag{13}$$

where,

R = the roots of equation 12

$\omega_i = \omega + \omega_a$ = the observed inflection points relative to the middle of each slope.

c = A variable unique for each slope inclination.

Equation 13 may be rewritten as:

$$x^n = c^n \omega^n \tag{14}$$

where,

ω = the dimensionless position anywhere in the slope relative to the middle of each slope.

Substituting equation 14 into equation 11 gives the following interslice side force functional relationship:

$$f(x) = e^{-\frac{1}{2}c^n \omega^n} \tag{15}$$

The computed values of 'c' and '$-\frac{1}{2}c^n$' for each slope inclination investigated are given in Table 2.

The vertical limits of the generalize function must also be defined. The magnitude of 'ω' at midslope is zero and the interslice side force ratio, X/E, would be computed as 1.0. Therefore, a variable 'K' must be introduced into equation 14 to displace the function vertically. Equation 14 now becomes:

$$f(x) = Ke^{-\frac{1}{2}c^n\omega^n} \tag{15}$$

where,

K = The magnitude of the interslice side force ratio, X/E, at midslope.

The value of K is defined as follows based on the finite element analyses.

$$K = \exp(D_i + D_s\ (\text{depth factor} - 1.0)) \tag{16}$$

where,

D_i = The natural logarithm of X/E intercepts corresponding to a depth factor of one as shown in Figure 8.

D_s = The slope of each line shown in Figure 8.

$$= \frac{\ln X/E_1 - \ln X/E_2}{\text{depth factor}_1 - \text{depth factor}_2}$$

Slope Inclination	n	R	$\omega_i = \omega_a + \omega$	c	$C = -\frac{1}{2}c^n$
3 : 1	6	$\pm$1.089	$\pm$1.588	0.686	-0.052
2 : 1	4	$\pm$1.107	$\pm$1.065	1.039	-0.583
1 : 1	2	$\pm$1.000	$\pm$0.576	1.737	-1.509
1 : 2	2	$\pm$1.000	$\pm$0.297	3.366	-5.664

TABLE 2 THE COMPUTED VALUES OF 'c' AND '$C = -\frac{1}{2}c^n$'

FOR EACH SLOPE INCLINATION

Figures 9a and 9b show the interslice side force ratio, X/E, at midslope versus the slope angle in degrees and the value of D_s versus the tangent of the slope angle. These two figures are used to obtain values of D_i and D_s for any given slope inclination.

COMPARISON OF THE GENERALIZED FUNCTION AND THE FINITE ELEMENT RESULTS

The distribution of the interslice side force ratios, X/E, computed by the functions based on the finite element method are shown in Figures 10a through 10e.

In general, the function closely matches the distribution of the interslice side force ratio, X/E, computed by the finite element method. A slight discrepancy is observed near the crest of each slope. In this region, the values of the interslice side force ratio, X/E, computed by the finite element method become slightly negative. This is attributed to tension caused by the influence of the boundary conditions and is considered incorrect. The value of X/E, should not become less than zero in this region and the proposed mathematical function is considered to give a better estimate of the interslice side force ratio X/E.

A poor correlation is observed in Figure 10d which shows the distributions of the interslice side force ratios for a deep seated slip surface within the 1:2 slope inclination. For this plot, the value of '$C = \frac{1}{2}c^n$' was computed to be -5.664 (see Table 2). However, using a value of 'C' equal to -2.000 gives a much improved correlation as shown in Figure 10e. Based on this observation, it is suggested that a value of 'C' equal to -2.000 be used for all steep slopes when considering deep seated slip surfaces.

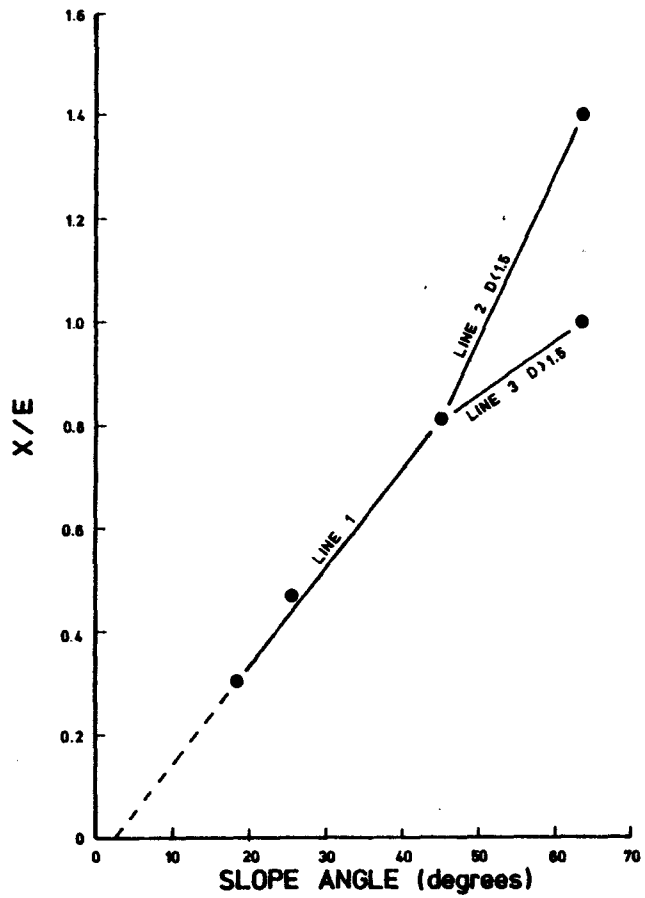

FIGURE 9a THE INTERSLICE SIDE FORCE RATIO (X/E) AT MIDSLOPE (DEPTH FACTOR = 1.0) VERSUS THE SLOPE ANGLE

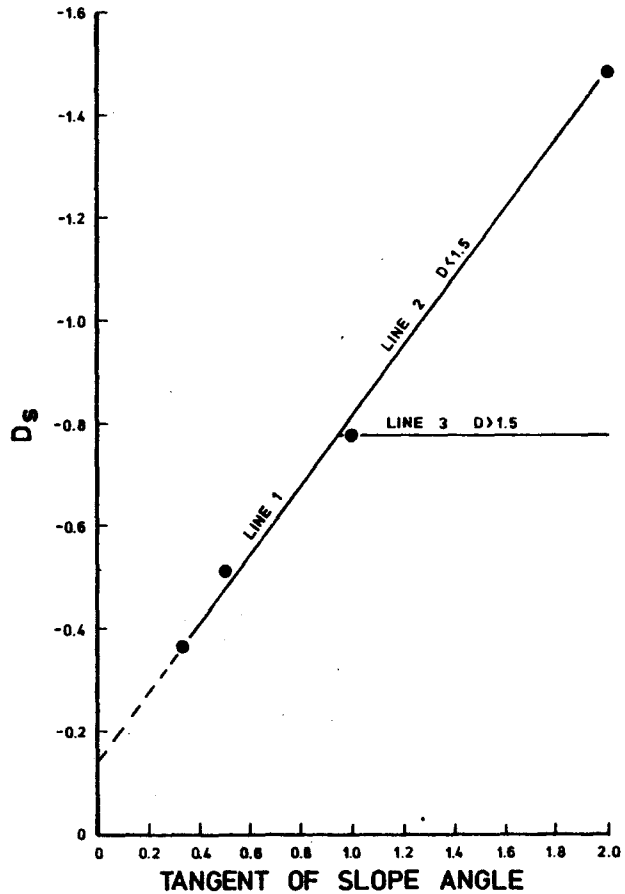

FIGURE 9b THE VALUE OF D_s VERSUS THE TANGENT OF THE SLOPE ANGLE

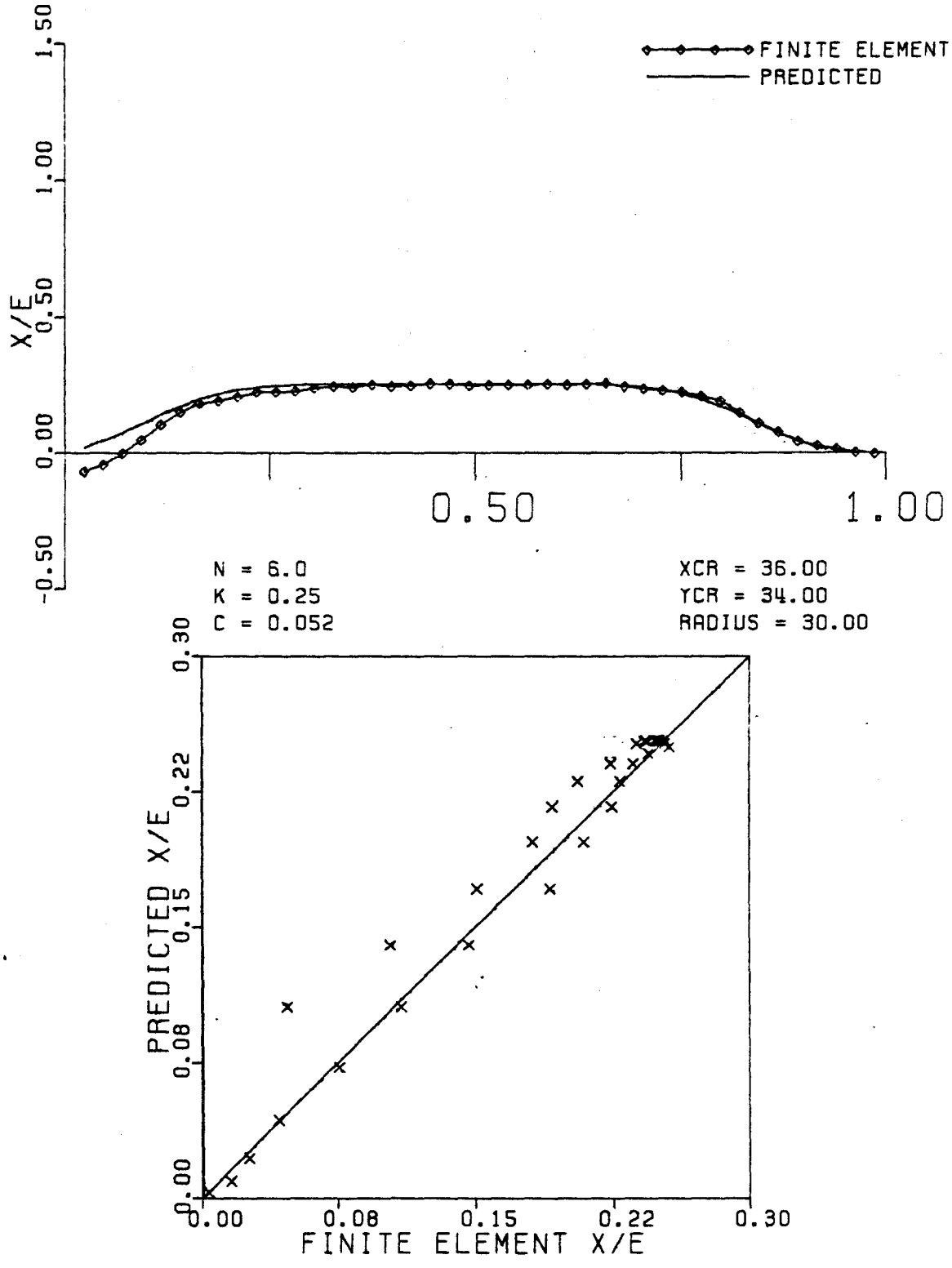

FIGURE 10a X/E COMPUTED BY THE GENERALIZED FUNCTION (PREDICTED) VERSUS X/E COMPUTED BY THE FINITE ELEMENT METHOD (DEEP SLIP SURFACE IN THE 3:1 SLOPE)

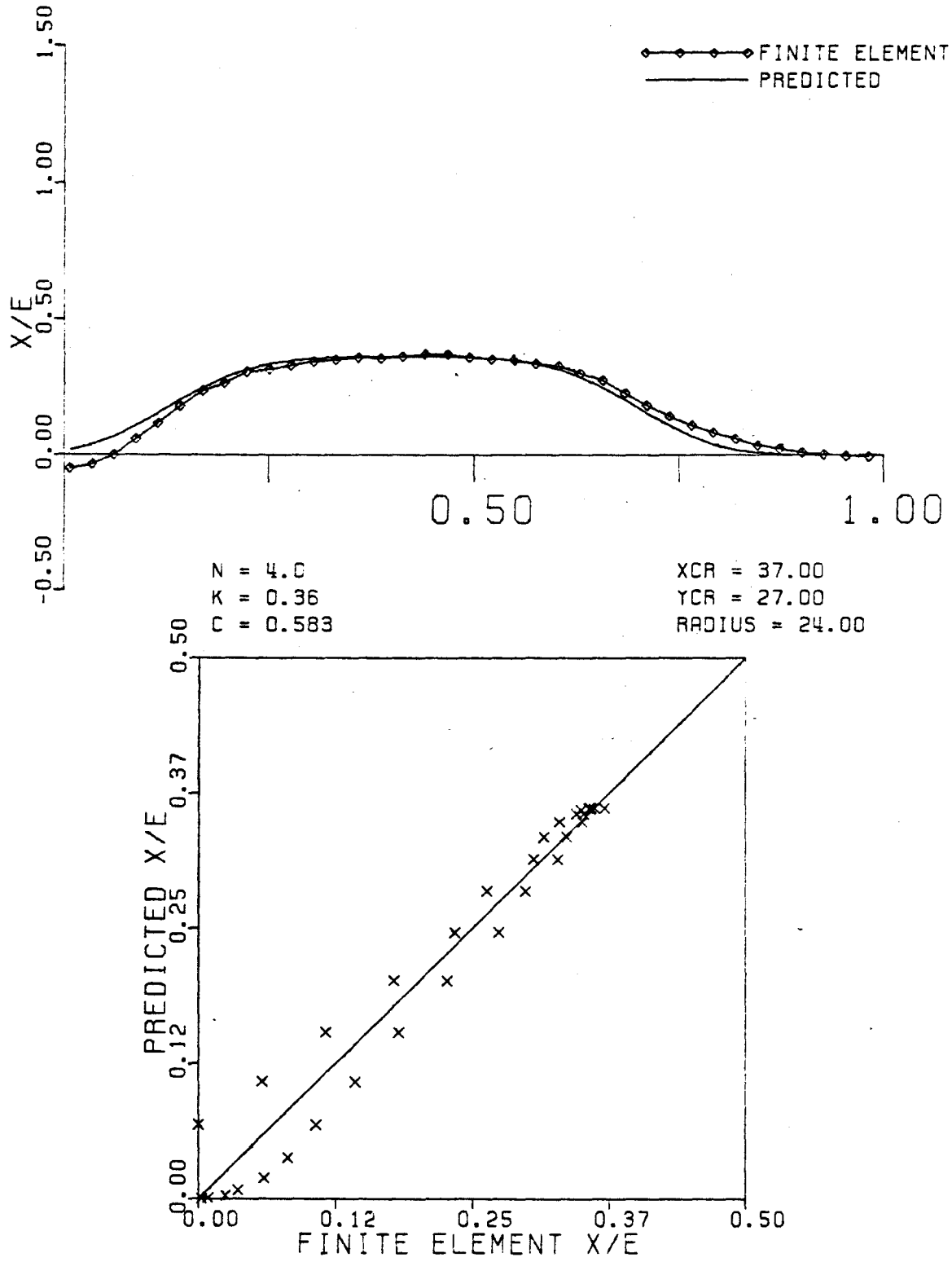

FIGURE 10b X/E COMPUTED BY THE GENERALIZED FUNCTION (PREDICTED) VERSUS X/E COMPUTED BY THE FINITE ELEMENT METHOD (DEEP SLIP SURFACE IN THE 2:1 SLOPE)

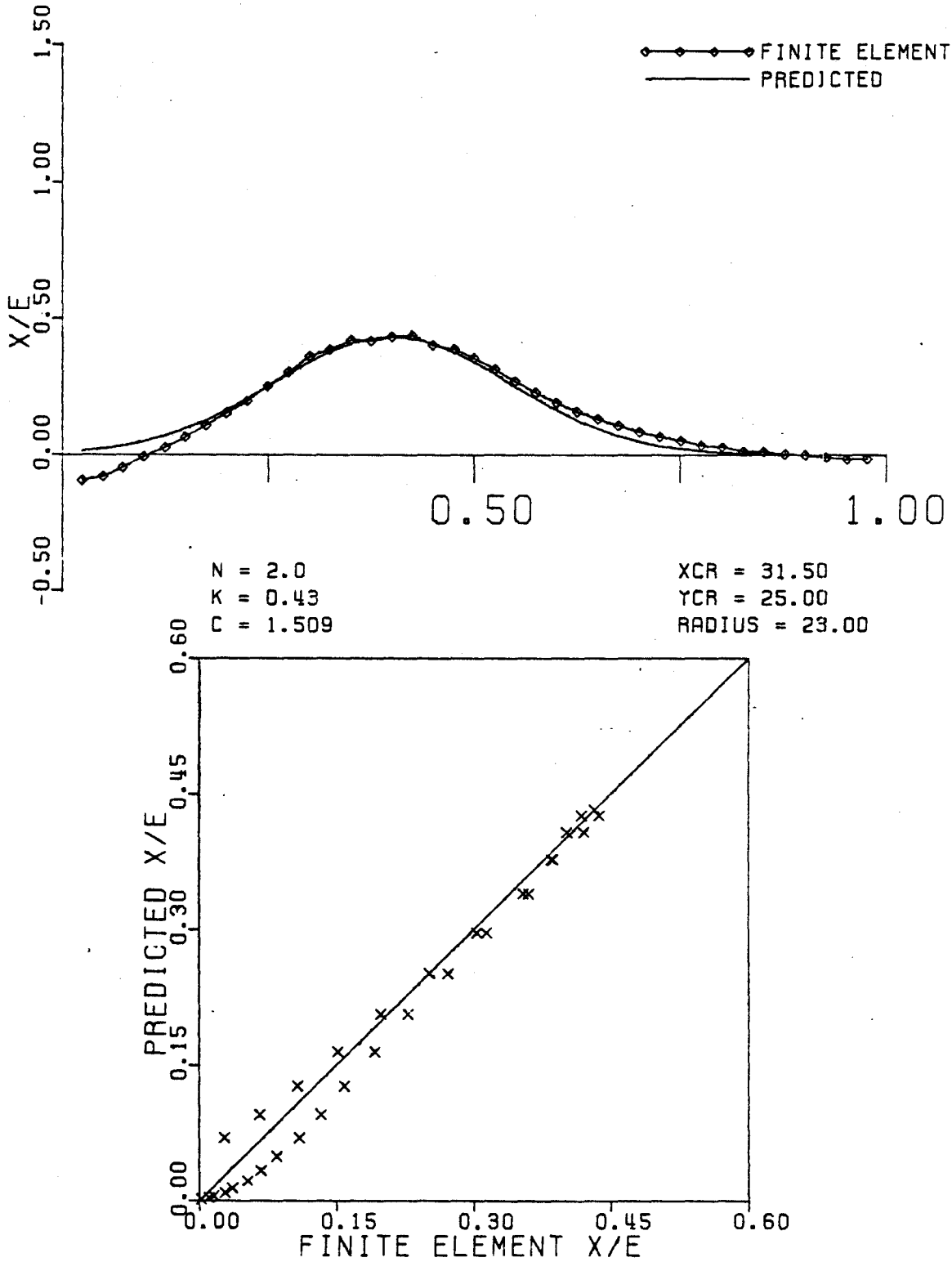

FIGURE 10c X/E COMPUTED BY THE GENERALIZED FUNCTION (PREDICTED) VERSUS X/E COMPUTED BY THE FINITE ELEMENT METHOD (DEEP SLIP SURFACE IN THE 1:1 SLOPE)

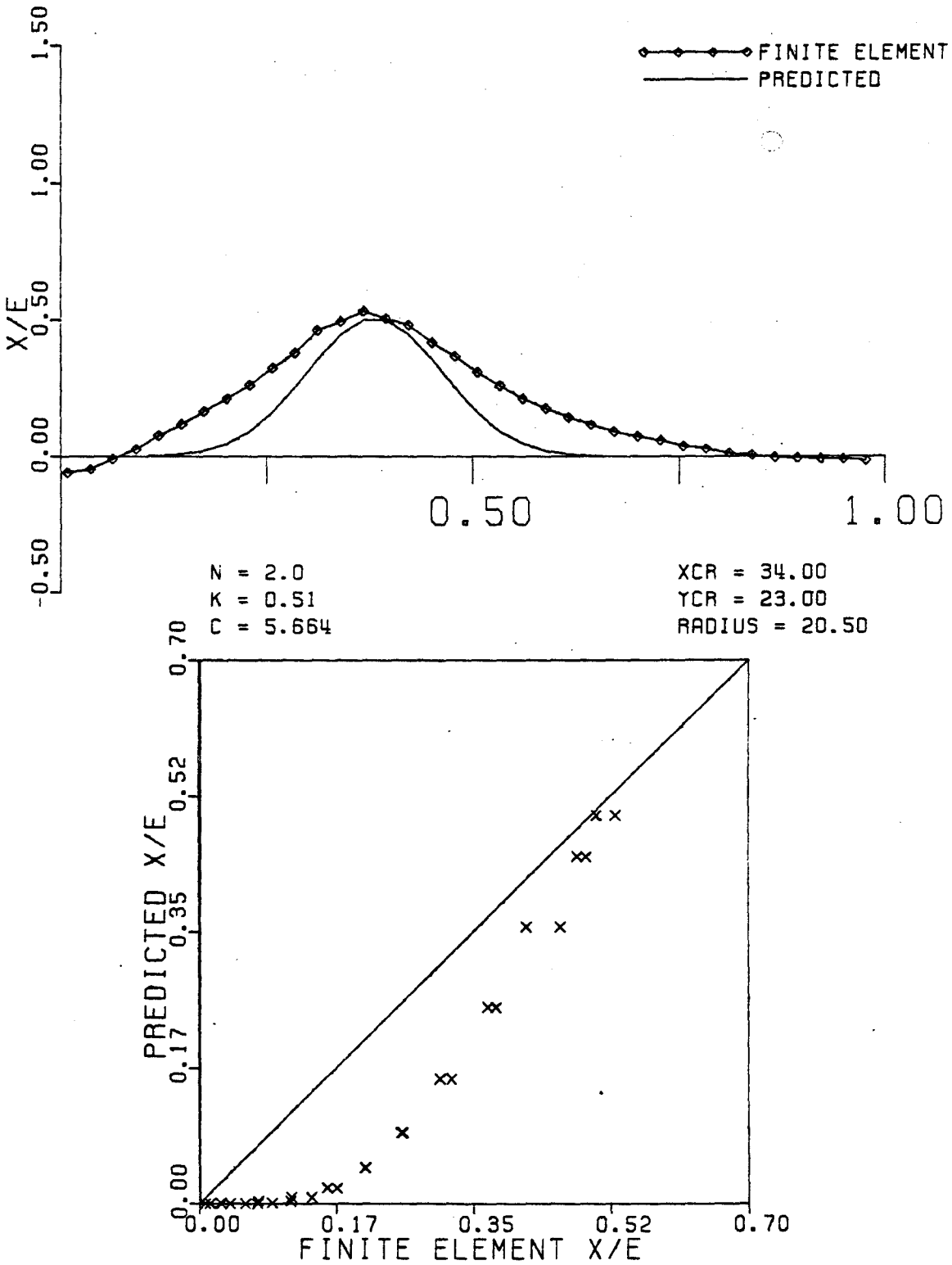

FIGURE 10d X/E COMPUTED BY THE GENERALIZED FUNCTION (PREDICTED) VERSUS X/E COMPUTED BY THE FINITE ELEMENT METHOD (DEEP SLIP SURFACE IN THE 1:2 SLOPE)

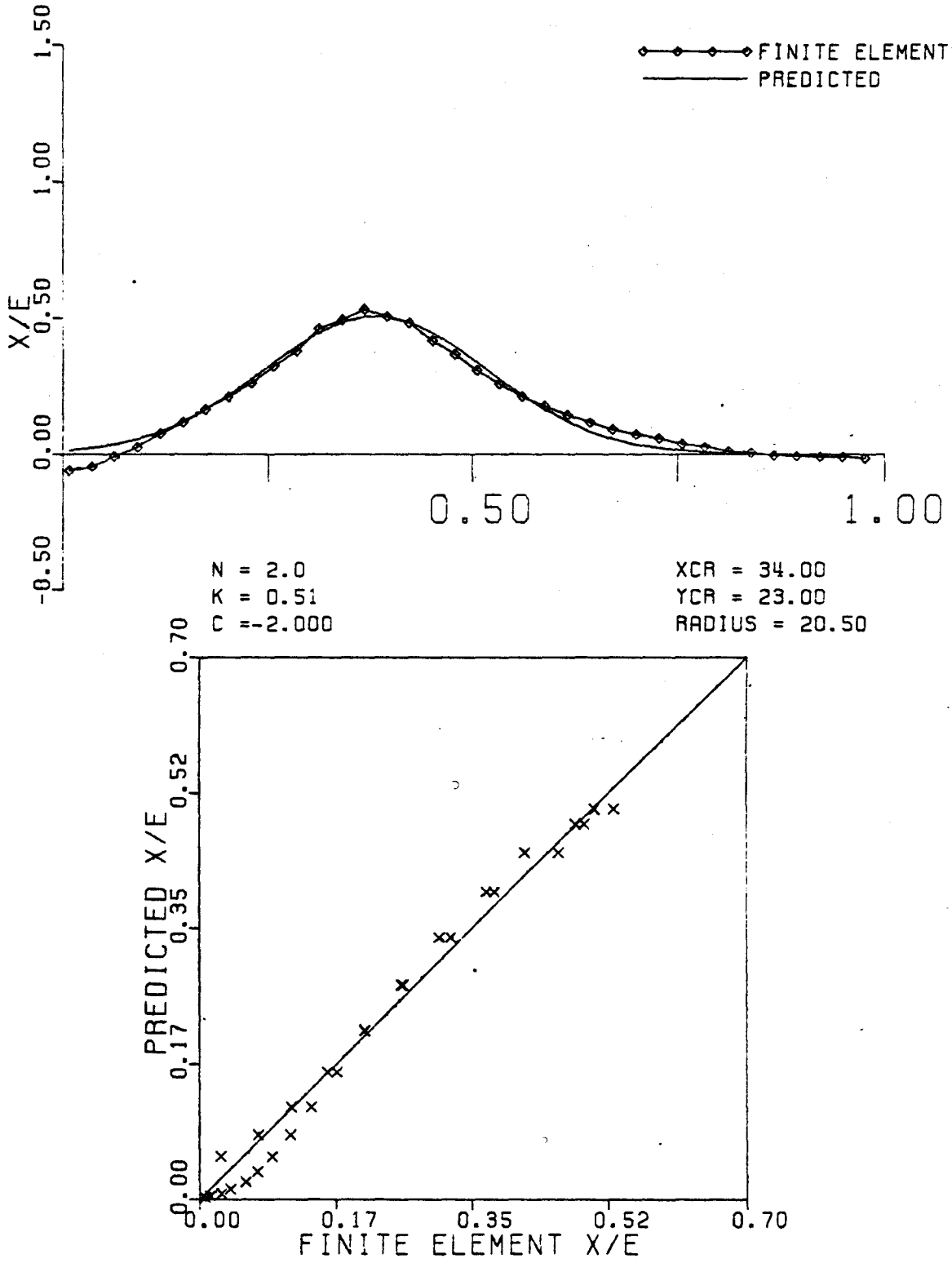

FIGURE 10e X/E COMPUTED BY THE GENERALIZED FUNCTION (PREDICTED) VERSUS X/E COMPUTED BY THE FINITE ELEMENT METHOD (DEEP SLIP SURFACE IN THE 1:2 SLOPE, SPECIAL CASE FOR 'C' = -2.000)

SUMMARY AND CONCLUSIONS

The distributions of the interslice side force ratio, X/E, for simple homogeneous slopes with circular slip surfaces have a characteristic shape. The distributions are bell-shaped. The bells are flattest for the 3:1 slope and sharpest for the 1:2 slope. Inflection points within the curvature of the distributions occur at approximately the breaks in slope at the crest and the toe of slope. These inflection points were observed to occur at an average distance equal to 0.069H beyond either the crest and toe of the slope. Finally, the maximum values of the interslice side force ratio, X/E, occurs at mid-slope between the crest and the toe of slope.

LIST OF REFERENCES

Bishop, A. W. (1955), "The Use of the Slip Circle in the Stability Analysis of Slopes", Geotechnique, Vol. 5, pp. 7-17.

Ching, R. K. H. (1981), "A Theoretical Examination and Practical Applications of The Limit Equilibrium Methods To Slope Stability Problems", M.Sc. Thesis, University of Saskatchewan, Saskatoon.

Desai, C. S. (1979), "Elementary Finite Element Method", Prentice - Hall, Inc., New Jersey.

Dunlop, P., Duncan, J. M. and Seed, H. B. , (1968), "Finite Element Analyses of Slopes in Soil", U.S. Army Engineer Waterways Experiment Station, Corps of Engineers, Vicksburg, Mississippi, Report No. TE 68-3.

Fredlund, D. G. (1978), "Two Dimensional Finite Element Program - Constant strain Triangle - User's Manual CD-2", Department of Civil Engineering, University of Saskatchewan, Saskatoon.

Fredlund, D. G., Krahn, J. and Pufahl, D. E. (1981), "The Relationship between Limit Equilibrium Slope Stability Methods", Proceedings of the Tenth International Conference on Soil Mechanics and Foundation Engineering, Stockholm.

Janbu, N. (1954), "Application of Composite Slip Surfaces for Stability Analysis", Proceedings of European Conference on Stability of Slopes, Vol. 3, pp. 43-49.

Morgenstern, N. R. and Price, V. E. (1967), "A Numerical Method for Solving the Equations of General Slip Surfaces", The British Computer Journal, Vol. 9, pp. 338-393.

Morgenstern, N. R. and Price, V. E. (1965), "The Analysis of the Stability of General Slip Surfaces", Geotechnique, Vol. 15, pp. 79-93.

Morgenstern, N. R. and Eisenstein, Z. (1970), "Methods of Estimation Lateral Loads and Deformations", Reprinted from, "Lateral Stresses and Earth Retaining Structures", Proceedings of ASCE Soil Mechanics and Foundations Division Specialty Conference held at Cornell University, June, 1970.

Sariano, A. (1976), "Iterative Schemes for Slope Stability Analysis", Numerical Methods in Geomechanics, Vol. 2, pp. 713-724.

Spencer, E. (1967), "A Method of Analysis of the Stability of Embankments Assuming Parallel Interslice Forces", Geotechnique, Vol. 17, pp. 11-26.

Spencer, E. (1973), "Thrust Line Criterion in Embankment Stability Analysis", Geotechnique, Vol. 23, pp. 85-100.

Stark, P. A. (1970), "Introduction to Numerical Methods", MacMillan Publishing Co., Inc., New York.

Toews, N. A. and Yu, Y. S. (1974), "A Computer Program for Mesh Generation for the 2-D Finite Element Program Wilax", Research Report R-272, Mines Branch, Dept. of Energy, Mines and Resources, Ottawa, Ontario.

Wang, F. D. and Sun, M.C. (1970), "Slope Stability Analysis by the Finite Element Stress Analysis and Limiting Equilibrium Method", Report 6F, US Bureau of Mines, R17341, Jan. 1970, 16P.

Whitman, R. V. and Bailey, W. A. (1967), "Use of Computer for Slope Stability Analysis", Journal of Soil Mechanics and Foundations, ASCE, Vol. 93, No. SM4, pp. 519-542.

Wright, S. G. (1969), "A Study of Slope Stability and Undrained Shear Strength of Clay Shales", PH.D. Thesis, Department of Civil Engineering, University of California, Berkeley.